

Upper critical field from normal state fluctuations in $\text{Bi}_2\text{Sr}_2\text{CuO}_{6+\delta}$

F. Bouquet, L. Fruchter, I. Sfar,* Z.Z. Li, and H. Raffy

Laboratoire de Physique des Solides, C.N.R.S. Université Paris-Sud, 91405 Orsay cedex, France

(Dated: Received: date / Revised version: date)

The in-plane magnetoresistance of an epitaxial $\text{Bi}_2\text{Sr}_2\text{CuO}_{6+\delta}$ thin film was systematically investigated as a function of doping, above T_c . We show evidence for a negative isotropic magnetoresistance for the most underdoped states, which we compare with the predictions from a Kondo mechanism. The positive orbital magnetoresistance is used to extract the crossover field line $H_{c2}^*(T)$ in the fluctuation regime. This field is found in good agreement with the upper critical field obtained from resistivity data below T_c , and exhibits a similar upward curvature, thus pointing toward the existence of a critical correlation length. The consequences regarding the nature of the resistive transition are discussed.

PACS numbers: 74.25.Dw, 74.25.Fy, 74.40.+k, 74.72.Hs, 74.78.Bz, 74.81.Bd

I. INTRODUCTION

The superconducting transition in a magnetic field of high- T_c cuprates has shown unusual features. Within a flux line description, the combined effects of high temperature, strong anisotropy, short coherence length and large penetration depth promotes a large flux liquid domain in the vicinity of the upper critical-field line, $H_{c2}(T)$. Such a liquid is characterized by the loss of the phase coherence, which is otherwise present in the ordered Abrikosov vortex lattice;¹ the first order flux melting transition (or the irreversibility line, in the case of disordered materials) replaces the usual superconducting transition, which is no longer characterized by the occurrence of zero resistivity. Early observations pointed out the importance of phase fluctuations below T_c .² The absence of a genuine transition opens the possibility to describe the ‘normal’ state as a region of fluctuating vortices. However, in the absence of local pairing, regular vortices do not survive above T_c . The observation of a large Nernst effect well above T_c , combined with a diamagnetic magnetization, has promoted the idea that phase alone is broken at the superconducting transition, while condensate amplitude remains finite.³ In the vortex description, this means that the vortex-core energy remains essentially unchanged at the superconducting transition and that it is unusually small. Therefore, the usual mirror in the descriptions of the fluctuating superconducting state and of the fluctuating normal state is broken: this results from the observation of an upper critical field which remains constant through T_c .^{3,4} Thus, experiments which are able to probe the upper critical field above and below T_c are valuable. In the following, we demonstrate that magnetoresistance measurements reveal a crossover field line $H_{c2}^*(T)$ above T_c which is essentially similar to the $H_{c2}(T)$ line below T_c . This suggests that both lines are governed by a common correlation length, as expected for a regular continuous transition.

II. EXPERIMENTS

Transport measurements were performed on one epitaxial, 2700 Å thick, *c*-axis oriented, $\text{Bi}_2\text{Sr}_2\text{CuO}_{6+\delta}$ ($\text{Bi}-2201$) thin film, which was grown on a heated SrTiO_3 substrate, using *rf* sputtering (Ref. 5 and refs. therein). The quality of the orientation is attested by the rocking curve through the (008) peak, which has a full width at half maximum less than 0.2°. It was patterned in the standard 5 points resistivity and Hall-effect measurements configuration, with a 160 μm long and 95 μm large strip. The sample was first annealed and slowly cooled in a pure oxygen flow at 420°C, yielding a non superconducting overdoped state. Successive lower-doped states were obtained by annealing the sample under vacuum, using temperatures between 240 and 290°C (Fig. 1). The evolution of doping was monitored using the conductivity at 300 K. Transition temperatures are defined at the midpoint of the resistive transition. The transition width (10% – 90% completion) of the optimally doped sample ($T_c \simeq 19$ K) was 2 K.

The resistivity was measured using a standard lock-in detection, with a 90 μA *ac* current. Hall measurements, used to evaluate the hole density, were performed with the same *ac* technique, reversing the magnetic field by a 180° rotation. Special care was taken to limit temperature shifts during measurements under a magnetic field: after stabilization of the temperature in zero magnetic field using a calibrated thermometer, the temperature measurement and regulation was switched to a capacitance sensor with virtually no magnetic dependence and the magnetic field was ramped. The temperature stability was better than 30 mK. For the angular measurements, the magnetic field could be rotated around an axis parallel to the transport current (Fig. 2). Using the minimum in the magnetoresistance (MR), we were able to align the magnetic field within the film plane (CuO_2 plane) to better than 1° to determine the longitudinal magnetoresistance.

III. RESULTS AND DISCUSSION

A summary of the raw MR data and the experimental configuration are given in Fig. 2. Clearly, the transverse magnetoresistance (TMR, $\theta = 0$) is found roughly *symmetric* with doping (the iso-MR curves roughly scale with the symmetric T_c). On the other hand, the longitudinal magnetoresistance (LMR, $\theta = \pi/2$) is *asymmetric* and is smaller on the underdoped side of the phase diagram. Moreover, the LMR is found negative for the two most underdoped samples. We now postulate that the MR originates from the sum of an isotropic conductance (independent of the magnetic field orientation) and an orbital one (which scales with field and angle according to the anisotropic mass law^{6,7}):

$$\sigma(\theta, H) = \sigma_{\text{orb}}(\tilde{H}) + \sigma_{\text{iso}}(H), \quad (1)$$

where $\tilde{H} = H [\cos(\theta)^2 + \gamma^2 \sin(\theta)]^{1/2}$ and $\gamma^2 < 1$ is the anisotropic mass ratio. So we have :

$$\sigma_{\text{orb}}(H) = \sigma(0, H) - \sigma(\pi/2, H) + \sigma_{\text{orb}}(\gamma H) \quad (2)$$

$$\sigma_{\text{iso}}(H) = \sigma(\pi/2, H) - \sigma(0, \gamma H) + \sigma_{\text{iso}}(\gamma H) \quad (3)$$

As is usually done, we have neglected the last term in Eqs. (2, 3) to obtain σ_{orb} and σ_{iso} from the LMR and TMR. We self-consistently checked that these terms are negligible. Within the two-dimensional approximation ($\gamma = 0$), the data for $H \parallel ab$ in Fig. 2 would directly correspond to the isotropic MR.

For the most underdoped sample, we obtain the anisotropic mass ratio in the following way: we first set $\sigma_{\text{iso}} \equiv 0$ and determine the γ value which scales the data $\sigma(\theta, H)$ at $H = 3$ T and $H = 6$ T, using Eq. (1). Then, using the LMR and TMR data, $\rho(0, H)$ and $\rho(\pi/2, H)$, the isotropic component is obtained as well as the orbital one. The scaling procedure is iterated taking into account the new orbital component until the γ value is consistent with the set of angular- and field-dependent MR data. As shown in Fig. 3, $\gamma^{-1} = 22 \pm 2$ scales the data nicely. We have used this anisotropy value to extract the isotropic and orbital component of the MR for all doping states.

The observation of a negative longitudinal in-plane magnetoresistance with a simultaneous positive transverse in-plane magnetoresistance demonstrates the isotropic character of the negative MR. This rules out an orbital origin for this contribution (as an orbital one would contribute as $\simeq \gamma^{-1} \times$ LMR to the TMR, which does not show up in Fig. 4). For the same reason, the origin of this negative MR can be found neither in the superconducting fluctuations (since the only negative contribution to the field-dependent excess conductivity is the anomalous Maki-Thompson orbital one, which is anisotropic⁷), nor in the two-dimensional weak localization (the latter was generally thought to explain the low-temperature upturn of the resistivity in the underdoped cuprates until the observation of a similar upturn in the transverse resistivity refuted this conventional picture⁸).

The present results contrast with the ones obtained on a heavily underdoped, nonsuperconducting, $\text{Bi}_2\text{Sr}_2\text{CuO}_6$ single crystal in Ref. 9. Indeed, based on the observation of a negative, *anisotropic* magnetoresistance, the authors interpreted the low-temperature resistivity upturn as the occurrence of weak two-dimensional localization. Our results for the most underdoped state clearly indicate that the magnetoresistance is here a balance between a *positive, anisotropic* contribution (likely due to superconducting fluctuations) and a *negative, isotropic* one, the former overcoming the latter as $T \rightarrow T_c$ (Fig. 2).

It is generally admitted that the isotropic MR originates from a spin effect. While a negative out-of-plane MR is naturally understood as the closing of the pseudogap by the magnetic field (at a characteristic field given by $g\mu_B H \approx k_B T^*$, where T^* is the temperature for the opening of the pseudogap¹⁰), the in-plane negative MR cannot be accounted by the same effect, as the opening of the gap in the spin excitation spectrum results in a decrease of the resistivity and a positive MR.⁸ Such a behavior may be expected from the Kondo mechanism. This was first proposed to account for the isotropic negative MR in both insulating and superconducting $\text{La}_{2-x}\text{Sr}_x\text{CuO}_{4+y}$ ¹¹ (similar isotropic negative magnetoresistance was reported in the case of $\text{Bi}_2\text{Sr}_2\text{Ca}_{0.8}\text{Y}_{0.2}\text{Cu}_2\text{O}_{8+\delta}$ ¹²). In the Kondo scenario, a crossover between a quadratic field dependence and a logarithmic one is expected when $k_B T = g\mu_B H_{\text{cr}}$, where $g = 2$ (from the generalized Hamann formula¹³ – or ‘KMHZ’ formula). However, in the references 11 and 12 the crossover field was found one order of magnitude smaller than this prediction. The same observation may be done in the present case, as we have $g\mu_B H_{\text{cr}}/k_B T \simeq 0.1$ (using $H_{\text{cr}} \simeq 1.5$ T at $T = 20$ K, Fig. 4). Consistently, attempts to fit the magnetoresistance using the KMHZ formula is possible only by using some effective magnetic field αH , where $\alpha \simeq 0.1$, and decreases with increasing temperature (Fig. 5). In Ref. 14, the low-temperature resistivity upturn for heavily underdoped, non superconducting $\text{La}_{2-x}\text{Ce}_x\text{CuO}_4$ was fitted using the KMHZ formula. While such a fit was found satisfying, the KMHZ formula similarly failed to properly describe the negative magnetoresistance, the discrepancy increasing with higher temperature (Fig. 5, inset). An alternative explanation may be looked for within a spin-glass scenario, since, as pointed out in Ref. 11, spin glasses also exhibit an isotropic negative magnetoresistance. There are indeed evidences for the occurrence of a spin glass system on the high-doping side of the antiferromagnetic phase, coexisting with the superconducting one (for a review, see Ref. 15). Metallic alloys exhibit a spin glass state between the very dilute situation, showing the Kondo effect, and the concentrated one, for which the ordered magnetic state (ferromagnetic or antiferromagnetic) is found. The glass state allows to account for a crossover field (actually, the exchange field) as small as the one observed here, as $k_B T_g \simeq \mu_B H_{\text{cr}}$, using $T_g \simeq 1$ K. However, this is valid only below the freezing temperature T_g . At temperature

higher than T_g the MR for these systems is quadratic up to a magnetic field much larger than H_{cr} ,^{16,17} which is clearly not observed here, ruling out the glass state scenario. A remarkable feature is the occurrence of a maximum of the negative MR at $T \simeq 20$ K (Fig. 4, inset). Such a behavior is usually observed in ordered antiferromagnets close to T_N . Here, this maximum likely points toward a balance between a reduction of the spin scattering due to increased AF correlations and an increase due to local Kondo interactions as the temperature is lowered. In other words, none of these mechanisms (Kondo or spin-glass) can precisely account for our data; however the observed maximum in T of the MR points more toward a magnetic ordering effect than toward a frozen magnetic disorder (as in a spin glass). Finally, it should be underlined that the negative magnetoresistance discussed above represents only a very small fraction of the low temperature resistivity upturn. Fits in Fig. 5 indicate that the magnetic field is very far from asymptotically exhausting this upturn, so that a possible Kondo effect for the negative magnetoresistance does not allow us to conclude that the upturn has the same origin.

We now proceed to the discussion of the orbital MR. Two contributions to the orbital magnetoresistance are expected: the Aslamazov-Larkin one (ALO) and the Maki-Thompson one (MTO). Since the MTO contribution is less singular than the ALO one, it is expected to overcome the ALO contribution only well above T_c , as verified experimentally.^{18,19} In this regime, the characteristic field of the MTO contribution is $H_\phi = \hbar/(4D e \tau_\phi)$, where D is the diffusion coefficient and τ_ϕ is the phase dephasing time.²⁰ Considering the optimally doped sample ($T_c = 18.3$ K) and $T \simeq 2T_c$, the Hall coefficient (taken at high temperature, where it is roughly constant) $R_H = 1.5 \cdot 10^{-9} \text{ m}^3/\text{C}$ allows to compute the two-dimensional Fermi vector $k_F = 5.7 \cdot 10^7 \text{ cm}^{-1}$. The resistivity being $\rho = 2.3 \cdot 10^{-6} \Omega \text{m}$, we compute the metallic parameter $k_F l = 14$. Using for the electron effective mass $m^* = 3m_e$,²¹ we get the diffusion coefficient, $D = \hbar k_F l/(2m) = 2.7 \cdot 10^{-4} \text{ m}^2/\text{s}$. Being in the linear resistivity regime, we may evaluate the dephasing rate as the thermal transport scattering rate, $\tau = 1.2 \cdot 10^{-14} \text{ s}$. From this, we evaluate the dephasing field $H_\phi = 50$ T. So, the contribution from the MTO process should be small in the range of field and temperature of interest and we shall neglect it (in addition, this correction, larger for larger temperature, should contribute to increase the magnetoresistance and cannot account for the curvature of the $H_{c2}^*(T)$ line discussed below). The formula describing this contribution generally assume a linear dependence in T for the characteristic field H_{c2}^* (which corresponds to a quadratic divergence of the coherence length near T_c). We used the more general formula of the ALO contribution where the temperature dependence for

$H_{c2}^*(T)$ is kept arbitrary:²²

$$\begin{aligned} \sigma_{\text{ALO}} &= -2\sigma_0 \epsilon^{-1} \Upsilon_{\text{ALO}}(H/H_{c2}^*(T)), \\ \Upsilon_{\text{ALO}}(x) &= \{[\psi(1+2/x) - \psi(1/2+2/x)]/x - 1\}/x, \\ \sigma_0 &= e^2/16\hbar s, \end{aligned} \quad (4)$$

where $s = 12.3 \text{ \AA}$ is the superconducting plane separation and $H_{c2}^*(T)$ is the crossover field, symmetric with respect to T_c of the upper critical field $H_{c2}(T)$. When $H \ll H_{c2}^*(T)$, the field dependence is quadratic and the magnetoconductance is, assuming $H_{c2}^*(T) = \epsilon H_{c2}^*(0)$ ($\epsilon = \ln(T/T_c)$):

$$\Delta \sigma_{\text{ALO}} \simeq -\sigma_0 H^2/2H_{c2}^*(0) \epsilon^3 \quad (5)$$

We do observe such a quadratic dependence at high temperature. A linear fit as in Fig. 6 ($T = 33$ K) straightforwardly provides the value $H_{c2}^*(33 \text{ K}) = 37 \pm 4$ T for the almost optimally doped sample. This agrees with the determination of the upper critical field from resistivity data in the limit $T \rightarrow 0$ presented in Ref. 23. However, it is seen that quadratic fits of the MR for larger temperature yields larger values of the upper critical field. This means that $H_{c2}^*(T)$ is not a linear function of ϵ as assumed in Eq. (5) and that it exhibits an upward curvature. This may be seen using the full expression in Eq. (4) to determine $H_{c2}^*(T)$. A convenient way to do this is to determine $H_{c2}^*(T)$ such that $\epsilon \Delta \sigma_{\text{orb}}$ vs $H/H_{c2}^*(T)$ obtained at different field and temperature values defines a single curve. As seen in Fig. 7, it is possible to reasonably scale the data along this scheme. The universal function in Eq. (4) roughly accounts for the scaled data. We have noticed, however, that for the strongly overdoped and underdoped states, the prefactor σ_0 in Eq. (4) – when used as a fitting parameter – is reduced by about 30% with respect to the theoretical value, which may result from a spread of the doping level. Also, at low temperature ($\epsilon < 0.1$), the universal function obtained in this way systematically deviates from Eq. (4), which could be due to the finite width of the transition or to the occurrence of critical fluctuations in the vicinity of T_c . The H_{c2}^* values needed to scale the data define a strongly curved $H_{c2}^*(T)$ line, the curvature being stronger for lower doping (Fig. 8). Given the reduced temperature and the transition temperature, the crossover field found in this way is also lower for the underdoped regime, which is a direct consequence of the excess MR on the underdoped side (Fig. 9). The excess MR cannot be due to the onset of localization, which would contribute as a negative MR. We have also checked, using the procedure described in Ref. 38, that the effect of T_c inhomogeneities is to depress the $H_{c2}(T)$ values obtained from our procedure only for temperatures such that $T - T_c \lesssim \Delta T_c$, where ΔT_c is the width of a Gaussian T_c distribution. So, a curvature for T larger than $2T_c$, as observed in the underdoped regime, cannot be accounted by such a distribution. The $H_{c2}^*(T)$ found in this way is strikingly similar to the one inferred from the onset of the resistive transition *below* T_c on a

similar sample,^{36,37} using the determination of Ref. 23 (Fig. 8).

There has been several interpretations for the upward curvature observed in various cuprates and organic materials (see Ref. 24 and refs therein). First, from an experimental point of view, it was pointed out that this might result from an incorrect determination of the upper critical field from resistive measurements. Indeed, the in-plane resistive transition might yield a considerably lower value than the true upper critical field, due to the existence of a large flux liquid regime above the melting line. In Ref. 25, it was found that, for strongly overdoped Bi-2201 single crystals, a regular $H_{c2}(T)$ line is obtained, provided that the resistive criterion is chosen close to the normal state resistivity value. Existence of similar thermally activated motion of pancake vortices was opposed to the critical field measurements from out-of-plane resistivity.²⁶ However, analysis of magnetization measurements on Bi-2201 showed that a linear dependence allows for the scaling of the magnetic moment with field and temperature, but that a power law ($\epsilon^{2.5}$) is needed to scale both the magnetic moment and its second derivative, $\partial^2 M / \partial T^2$.²⁷ Concerning theories, it was argued in Ref. 28 that the curved $H_{c2}(T)$ obtained from out-of-plane resistivity is intrinsically related to the superconducting mechanism in cuprates. According to these authors, this curvature is consistent with the predictions based on the Bose-Einstein condensation of bosons formed above T_c . It was argued that this model is unable to account for the observation of similar data for overdoped samples, whereas this could be explained within the Boson-Fermion model, which accounts for both real-space paired carriers and itinerant Fermions.²⁹ In Refs. 30,31, a peculiar magnetic pair-breaking mechanism specific to two-dimensional superconductors, allowing both strong pair-breaking effects and a clean situation, was shown to correctly describe the $H_{c2}(T)$ features. Finally, it was proposed that the critical field obtained from resistivity is actually the place of phase ordering of superconducting grains imbedded in the material (with a critical temperature higher than the zero-field resistivity one);^{32,33} above this field, decoupled grains with non-zero superconducting order parameter would subsist. This mechanism could be either intrinsic to these cuprates for which there is a local doping effect,³⁴ or could originate from chemical inhomogeneities or substitutions due to the elaboration process.

Our data obtained *above* the zero field transition temperature confirm this curvature. This rules out a conventional flux-flow mechanism as the origin of the anomalous $H_{c2}(T)$ curvature. More generally, the observation of symmetric lines in the superconducting and the fluctuation regimes points toward the existence of a conventional correlation length similar to that obtained from the theory of second-order phase transitions (defined as $\xi^2 = \hbar / (2eH_{c2})$). We note that Nernst-effect measurements may also be used to define symmetric crossover lines. Such measurements locate the $H_{c2}(T)$ line ob-

tained from resistivity measurements as a crossover between the melting line and the ridge line joining points of maxima of the Nernst signal vs H .³ A ridge line may also be found in the fluctuation regime above T_c from the data in Fig. 13 of Ref. 3: this line is found roughly symmetric with respect to T_c and may indicate the existence of a similar crossover line in the fluctuation regime. Such a behavior is not expected from a scenario where the resistive crossover would mark the loss of phase coherence, due to the proliferation of unbound vortices above T_c (see Ref. 39 and Refs. therein). Indeed, one may question in the present case the pertinence of the Kosterlitz-Thouless mechanism for this relatively weakly anisotropic material, over a temperature domain as large as $2T_c$, while experimental evidences for such a transition have pointed out mean field transition temperatures only a few kelvins above T_c (see e.g. Ref. 40). Alternatively, in 3D, the critical temperature region where the mean-field behavior is expected to break down is very narrow for this compound³⁵ and cannot account for the large temperature interval where the $H_{c2}(T)$ line is anomalous. Such a restriction might not hold in the case where only phase is broken; in such a case, the correlation length to be considered would be that of the phase coherence.

As underlined above, it appears that the transition is less robust to the magnetic field on the underdoped regime than it is on the overdoped one: the curvature for $H_{c2}^*(T)$ appears to be stronger for the underdoped states (this is best evidenced in Fig. 8, by comparing the overdoped state with $T_c = 11.6$ K to the corresponding underdoped state with $T_c = 12.1$ K). The origin of this asymmetry, either extrinsic (such as an increased disorder) or intrinsic (such as the proximity of the antiferromagnetic phase) is not known. In our case, it is seen to go along with the isotropic negative MR, which may indicate a contribution of magnetism. Such a contribution of a pair-breaking effect was proposed to account for the anomalous $H_{c2}(T)$ line in Ref. 30. We note that this mechanism ultimately leads to gapless behavior, recalling the pseudogap that supplants the true superconducting gap, when going over to the underdoped regime.

IV. CONCLUSION

We have investigated the magnetoresistance for a $\text{Bi}_2\text{Sr}_2\text{CuO}_{6+\delta}$ thin film, from highly overdoped to highly underdoped states above the zero-field resistive superconducting transition temperature. The isotropic magnetoresistance is found negative for the lower (but still superconducting) doping states, which we tentatively interpret as a Kondo mechanism. The orbital positive magnetoresistance is fitted by the Aslamazov-Larkin theory. This yields an anomalous critical-field temperature dependence, which agrees with previous resistive measurements below T_c . This points toward the existence of a similar correlation length above and below T_c , as expected for a continuous transition. The enhanced cur-

vature on the underdoped side indicates the existence of an additional mechanism that contributes to decrease of the phase stiffness.

Acknowledgments

We acknowledge the support of CMCU to Project No. 01/F1303.

-
- * Also at L.P.M.C., Département de Physique, Faculté des Sciences de Tunis, campus universitaire 1060 Tunis, Tunisia.
- ¹ A. K. Nguyen and A. Sudbø, Phys. Rev. B **58**, 2802 (1998).
- ² H. Raffy, S. Labdi, O. Laborde and P. Monceau, Physica C **184**, 159 (1991).
- ³ Yayu Wang, Lu Li and N. P. Ong, cond-mat/0510470 (2005).
- ⁴ Yayu Wang, S. Ono, Y. Onose, G. Gu, Yoichi Ando, Y. Tokura, S. Uchida and N. P. Ong, Science **299**, 86 (2003).
- ⁵ Z.Z. Li, H. Rifi, A. Vaures, S. Mgeert and H. Raffy, Physica C **206**, 367 (1993).
- ⁶ G. Blatter, V.B. Geshkenbein and A.I. Larkin, Phys. Rev. Lett. **68**, 875 (1992).
- ⁷ A. Larkin and A. Varlamov, 'Theory of fluctuations in superconductors', Clarendon Press, Oxford, chap. 8 (1969).
- ⁸ Yoichi Ando, G. S. Boebinger, A. Passner, Tsuyoshi Kimura and Kohji Kishio, Phys. Rev. Lett. **75**, 4662 (1995).
- ⁹ T.W. Jing, N.P. Ong, T.V. Ramakrishnan, J.M. Tarascon and K. Remschnig, Phys. Rev. Lett. **67**, 761 (1991).
- ¹⁰ T. Shibauchi, L. Krusin-Elbaum, Ming Li, M.P. Maley and P.H. Kes, Phys. Rev. Lett. **86**, 5763 (2001).
- ¹¹ N.W. Preyer, M.A. Kastner, C.Y. Chen, R.J. Birgeneau and Y. Hidaka, Phys. Rev. B **44**, 407 (1991).
- ¹² D. Thopart, A. Wahl, A. Maignan and Ch. Simon, Phys. Rev. B **62**, 5378 (2000).
- ¹³ H. Keiter, E. Müller-Hartmann and J. Zittartz, Solid State Commun. **16**, 1247 (1975).
- ¹⁴ Tsuyoshi Sekitani, Michio Naito and Noburu Miura, Phys. Rev. B **67**, 174503 (2003).
- ¹⁵ M.A. Kastner and R.J. Birgeneau, Rev. Mod. Phys. **70**, 897 (1998).
- ¹⁶ A.K. Nigam and A.K. Majumdar, Phys. Rev. B **27**, 495 (1983).
- ¹⁷ P.G.N. de Vegvar, L.P. Levy and T.A. Fulton, Phys. Rev. Lett. **66**, 2380 (1991).
- ¹⁸ S. Hikami and A.I. Larkin, Mod. Phys. Lett. B **2**, 693 (1988).
- ¹⁹ Y. Matsuda, T. Hirai, S. Komiyama, T. Terashima, Y. Bando, K. Iijima, K. Yamamoto and K. Hirata, Phys. Rev. B **40**, 5176 (1989).
- ²⁰ A.I. Larkin, JETP Lett. **31**, 219 (1980).
- ²¹ A. A. Tsvetkov, J. Schutzmann, J. I. Gorina, G. A. Kalushnaia, and D. van der Marel, Phys. Rev. B **55**, 14 152 (1997).
- ²² E. Abrahams, R.E. Prange and M.J. Stephen, Physica **55**, 230 (1971).
- ²³ M. S. Osofsky, R. J. Soulen, Jr., S. A. Wolf, J. M. Broto, H. Rakoto, J. C. Ousset, G. Coffe, S. Askenazy, P. Pari, I. Bozovic, J. N. Eckstein and G. F. Virshup, Phys. Rev. Lett. **71**, 2315 (1993).
- ²⁴ A.P. Mackenzie, S.R. Julian, G.G. Lonzarich, A. Carrington, S.D. Hughes, R.S. Liu and D.C. Sinclair, Phys. Rev. Lett. **71**, 1238 (1993).
- ²⁵ S. I. Vedeneev, A. G. M. Jansen, E. Haanappel and P. Wyder, Phys. Rev. B **60**, 12467 (1999).
- ²⁶ A.E. Koshelev, Phys. Rev. Lett., **76**, 1340 (1996).
- ²⁷ E. Janod, Thesis. Université Joseph Fourier - Grenoble I (1996).
- ²⁸ A.S. Alexandrov, V.N. Zavaritsky, W.Y. Liang and P.L. Nevesky, Phys. Rev. **76**, 983 (1996).
- ²⁹ Tadeusz Domski, Maciej M. Maśka and Marcin Mierzejewski, Phys. Rev. B **67**, 134507 (2003).
- ³⁰ Yu. N. Ovchinnikov and V.Z. Kresin, Phys. Rev. B **52**, 3075 (1995).
- ³¹ Yu. N. Ovchinnikov and V.Z. Kresin, Europhys. Lett. **46**, 794 (1999).
- ³² B. Spivak and F. Zhou, Phys. Rev. Lett. **74**, 2800 (1995).
- ³³ V.B. Geshkenbein, L.B. Ioffe, A.J. Millis, Phys. Rev. Lett. **80**, 5778 (1998).
- ³⁴ K. McElroy, Jinho Lee, J.A. Slezak, D.-H. Lee, H. Eisaki, S. Uchida and J.C. Davis, Science **309** 1048 (2005).
- ³⁵ L. Fruchter, I. Sfar, F. Bouquet, Z.Z. Li and H. Raffy, Phys. Rev. B **69**, 144511 (2004).
- ³⁶ H. Rifi, Z.Z. Li, S. Mgeert, H. Raffy, O. Laborde and P. Monceau, Physica C **235-240**, 1433 (1994).
- ³⁷ H. Rifi, Thesis. Université Paris Sud, Orsay (1996).
- ³⁸ A. Pomar, M.V. Ramallo, J. Mosqueira, C. Torrón and Félix Vidal, Phys. Rev. B **54**, 7470 (1996).
- ³⁹ J. Corson, R. Mallozzi, J. Orenstein, J.N. Eckstein and I. Bozovic, Nature **398**, 221 (1999).
- ⁴⁰ D.H. Kim, A.M. Goldman, J.H. Kang and R.T. Kampwirth, Phys. Rev. B **40**, 8834 (1989).

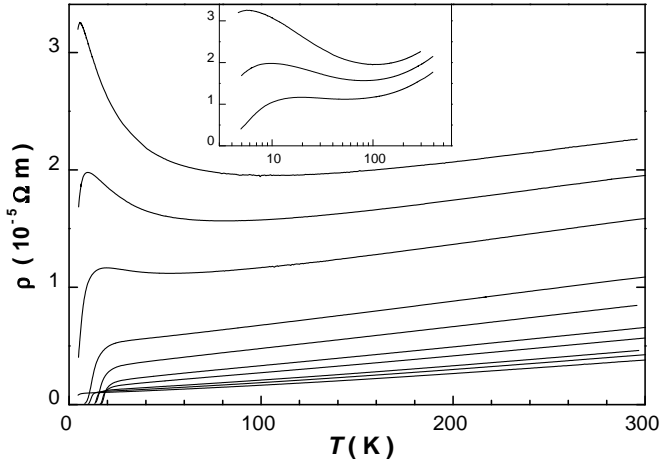


FIG. 1: Resistivity in zero field for the doping states displayed in Fig. 2. Inset, the three most underdoped states, in a semi-log representation.

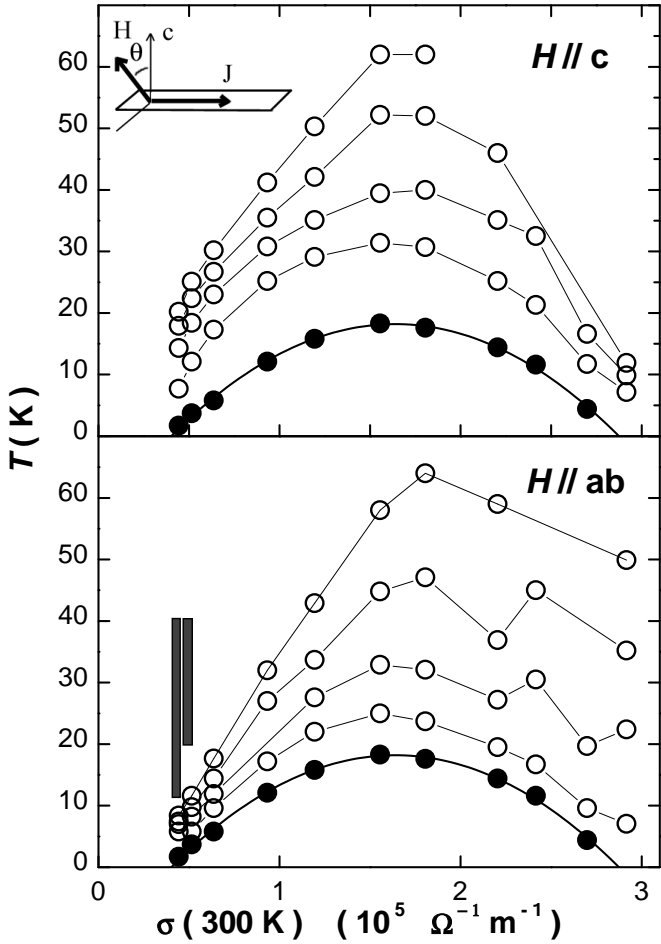


FIG. 2: Raw MR data ($H = 6$ T) for field applied perpendicular and parallel to the plane direction. Full circles: T_c (the line is a parabolic fit). Open circles: the temperature where the MR reaches a given criterion ($9.5 \cdot 10^{-3}$, $1.9 \cdot 10^{-2}$, $4.7 \cdot 10^{-2}$, and $0.19 \sigma_0$ from top to bottom). Shaded: area where a negative MR is observed.

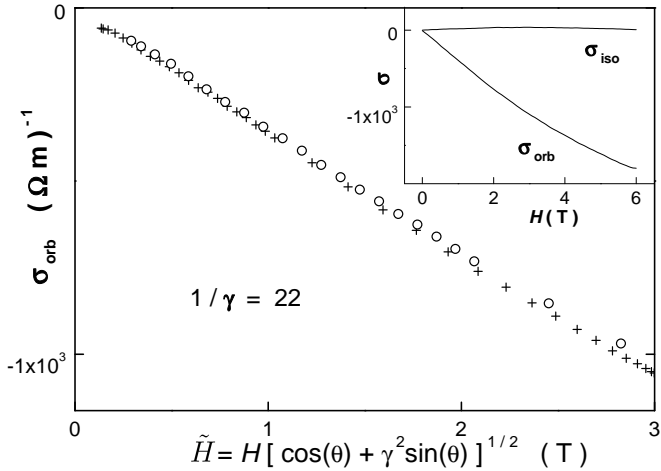


FIG. 3: Scaling of the orbital magnetoconductance ($T = 9$ K, $H = 3$ T and $H = 6$ T, $0 \leq \theta \leq \pi/2$) for the most underdoped sample, using the anisotropic mass law and $\gamma^{-1} = 22$. The inset shows the isotropic and orbital magnetoresistance, as determined by the iterative procedure.

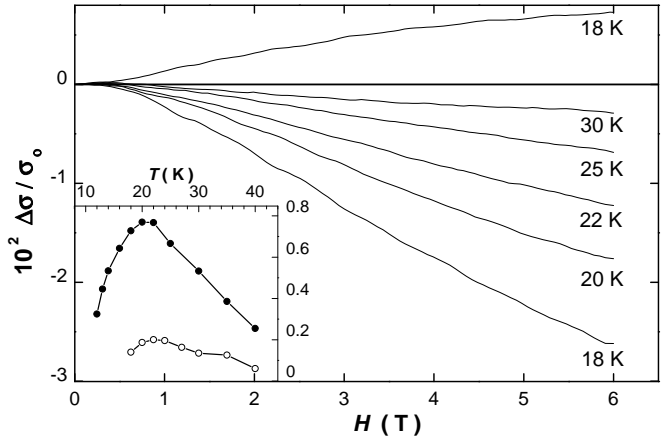


FIG. 4: Isotropic (positive) and orbital (negative) magnetoconductance for the most underdoped sample. The inset shows the isotropic magnetoconductance at 6 T (filled and open symbols are for the most and second most underdoped state in Fig. 2 respectively).

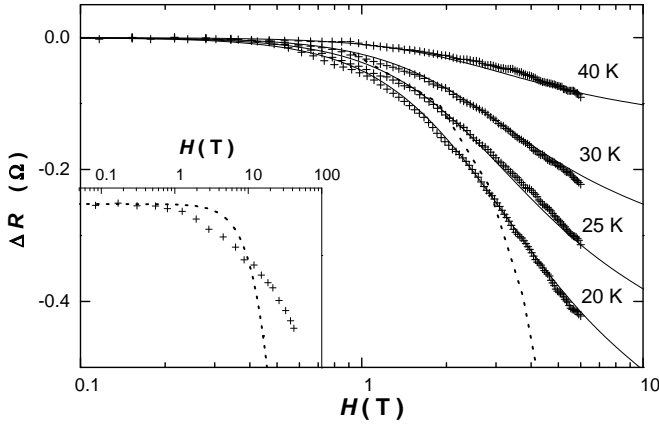


FIG. 5: Attempt to fit the parallel magnetoresistance, using the KMHZ formula and an effective magnetic field αH ($\alpha = 0.11, 0.06, 0.05, 0.037$ for $T = 20, 25, 30, 40$ K respectively). The dotted line is an attempt to fit the 20 K data, using $\alpha = 1$. Inset : magnetoresistance for heavily underdoped $\text{La}_{2-x}\text{Ce}_x\text{CuO}_4$ ($T = 20$ K) from Ref. 14. The dotted line is KMHZ formula, using the same parameters as in Ref. 14.

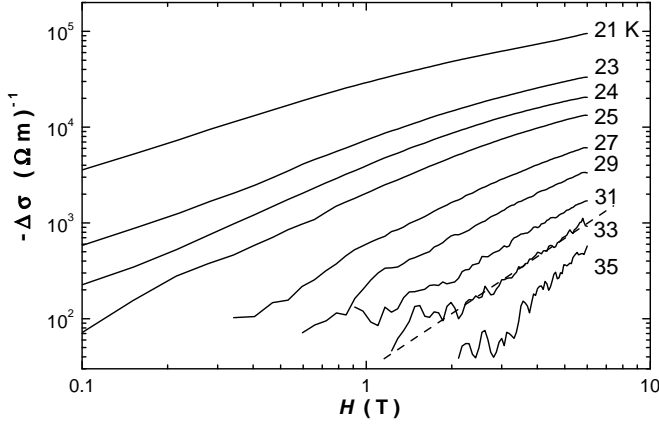


FIG. 6: Magnetoconductance for the almost optimally doped state with $T_c = 18.3$ K. The dashed line has slope 2.

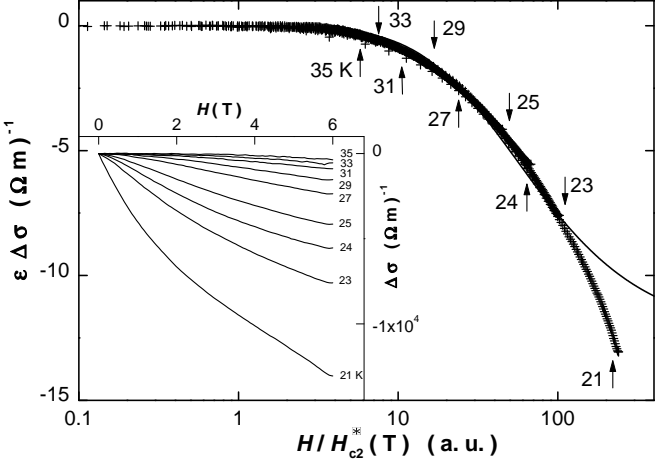


FIG. 7: Same data as in Fig. 6, rescaled according the ALO expression in Eq. (4) (line). The deviation from Eq. (4) (line) is observed at $T \lesssim 21$ K and $H \gtrsim 3$ T. Arrows indicate the location of the $H = 6$ T point.

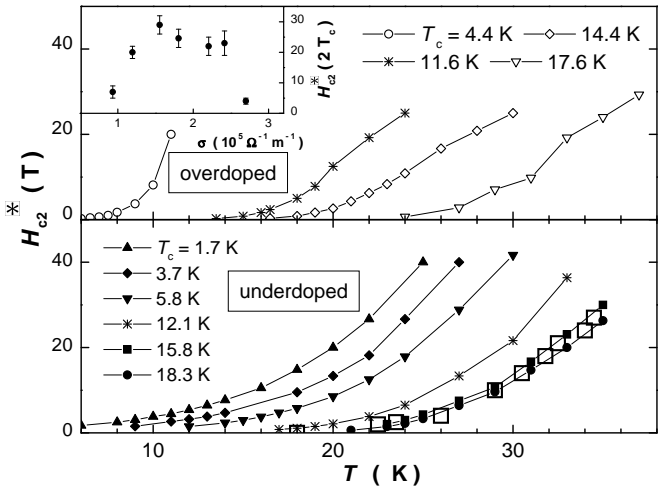


FIG. 8: Crossover field, from the scaling of $\epsilon \Delta \sigma_{\text{orb}}$. Open squares are obtained from resistivity below T_c for a thin film with $T_c = 16.5$ K,³⁷ following a mirror symmetry around T_c .

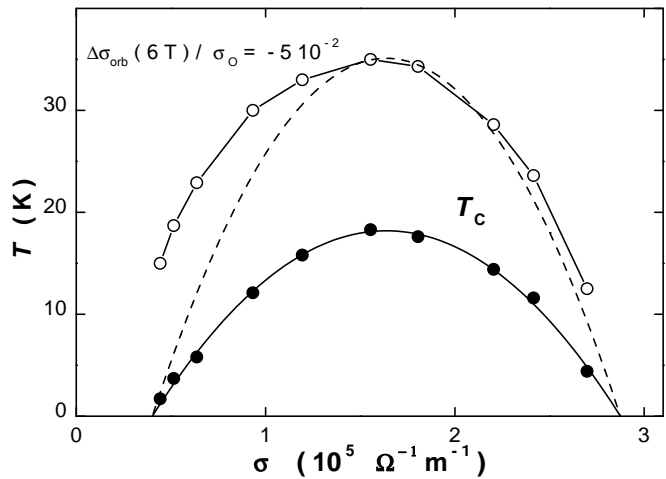


FIG. 9: Excess positive orbital MR for underdoped samples.
The full and dotted lines are homothetic parabolas.